Supporting Information

Two-Second Surface-confined Reconstruction of Cellulose Paper via a Recyclable Molten Salt Hydrate for Water-resistant Bioplastics

Ping Wang [a, b, †], Zhonglei Huang [b, †], Meiyan Wu [b], Safoora Mirmohamadsaghi [c], Chao Liu [b], Guang Yu [b], Haishun Du [d, *], Jing Shen [a, e, *], Bin Li [b, *]

[a] Research Division for Sustainable Papermaking & Advanced Materials, Key Laboratory of Biobased Materials Science and Technology of Ministry of Education, Northeast Forestry University, Harbin 150040, China
[b] Qingdao New Energy Shandong Laboratory, System Integration Engineering Center, Qingdao Institute of Bioenergy and Bioprocess Technology, Chinese Academy of Sciences, Qingdao 266101, China
[c] Department of Biotechnology, Faculty of Biological Science and Technology, University of Isfahan, Isfahan 81746-73441, Iran
[d] Department of Forestry, Michigan State University, East Lansing, 48824, USA
[e] Limerick Pulp and Paper Centre, Department of Chemical Engineering, University of New Brunswick, Fredericton, NB E3B 6C2, Canada

Corresponding authors' E-mail addresses: hdu@msu.edu (H. Du), jingshen@nefu.edu.cn, Jing.Shen@unb.ca (J. Shen), libin@qibebt.ac.cn (B. Li)

[†] The first two authors contributed equally.

Experimental characterizations

The Fourier Transform Infrared-Attenuated Total Reflection (FTIR-ATR) spectra of FP and MFP_{120}-2 samples were recorded using a spectrometer (Thermo Fisher, Nicolet 6700, USA) in the range of 4000–1500 cm^{-1}. Each sample was subjected to 64 scans, and the hydrogen density of the samples were calculated based on the previous literature.[1-3] Furthermore, the morphologies of FP and MFP samples were observed using a scanning electron microscope (SEM, Hitachi S-4800, Japan) with the acceleration voltage of 3 kV. In addition, X-ray photoelectron spectroscopy (XPS) spectra of FP and MFP_{120}-2 samples were collected using a spectrometer (Shimadzu, AXIS SUPRA+, Japan) at an analyzer pass energy of 100 eV. The morphology of MFP_{120}-2 sample was examined by a high-resolution transmission electron microscope (TEM, H-7600, Hitachi, Tokyo, Japan) at an accelerating voltage of 80 kV. The X-ray Diffraction (XRD) patterns of FP and MFP samples were collected on a diffractometer (Bruker, D8-Advance, Germany) with Ni-filtered Cu Kα radiation (λ = 1.5406 Å) at 40 kV and 40 mA. The range of scattering angle (2θ) was from 5 to 60º with a scanning step size of 0.02º and a scanning rate of 4 º·min^{-1}. The crystallinity index of the sample was estimated according to Segal's method using the Equation (1).[4]

$$CrI = \frac{I_{200} - I_{am}}{I_{200}} \times 100 \quad (1)$$

Where, I_{200} represents the maximum intensity of lattice diffraction from the main (200) peak, I_{am} values for cellulose are the minimum diffraction intensities observed between the plane reflections (110)/(200) and (1-10)/(110), respectively. For amorphous cellulose, the I_{am} values are selected as the peak intensities corresponding to the maximum value of the first-order derivative.[5]

Tensile properties of FP and MFP samples (50 mm × 10 mm) were measured at 25 ºC and 50% relative humidity (RH) using a universal testing machine (MTS Systems, CMT 6503, China) equipped with a 1000 N load cell at a crosshead speed of

5 mm·min^{-1}, following the TAPPI T497 standard. Wet tensile strength measurements were conducted in accordance with TAPPI T456. Each sample was tested 5 times, and the reported values represent the mean ± standard deviation.

The water contact angle of FP and MFP samples were conducted using a contact angle goniometer (KINO, SL200B, USA) at 25 ºC under 50% RH. The solvent resistance of MFP_{120}–2 was further evaluated by immersion in various organic solvents, including ethanol, isopropanol, acetone, tetrahydrofuran, and dimethylformamide and the morphology before and after a week of immersion was recorded at 25 ºC. FP and MFP_{120}-2 samples were immersed in deionized water (DI water). The samples were taken out daily, surface moisture was wiped off, and the weight was measured immediately. The water absorption rates of the films were calculated using the Equation (2).

$$Water\ absorption\ rate = \frac{M_1 - M_0}{M_0} \times 100\% \quad (2)$$

Where, M_1 and M_0 are the mass of films after and before immersion in water, respectively.

The thermogravimetric analysis (TGA) of FP and MFP_{120}-2 samples were detected by a TG-DSC analyzer (NETZSCH, STA 449F5 Jupiter, USA) from 50 to 600 ºC with a heating rate of 10 ºC·min^{-1} in a nitrogen atmosphere (25 mL·min^{-1}).

The oxygen transmission rate (OTR) of MFP_{120}-2 sample was tested using an OTR tester (Jinan Labthink, VAC-V2, China) at 25 ºC under 0% RH based on the ISO 2556:2001 standard. A round film with a diameter of 50 mm^2 was placed on a tester and sealed under vacuum for 8 h. Coefficient of thermal expansion (CTE) of FP and MFP_{120}-2, poly(lacticacid) (PLA), polyethylene (PE), polyurethane (PU) and polypropylene (PP) samples were detected by a thermomechanical analyzer (TMA450(EM)) from –20 ºC to 160 ºC with a heating rate of 10 ºC·min^{-1}.[6]

In addition, the biodegradability of the films was tested using two methods, i.e. landfill and compost biodegradation, respectively. The landfill biodegradation tests of

the films were conducted in the City of Qingdao (China) from October to November (Winter test).[7] Briefly, the films were cut into round pieces with length of 40 mm and width of 40 mm, and then were buried in natural soil at a depth of 10 cm. These samples were taken regularly for observation, and the mass loss of samples was also calculated. The compost biodegradation tests were carried out based on the previous report.[8] Briefly, the waste matrix was obtained by mixing 40% wood chip, 30% rabbit feed, 10% ripe compost, 10% corn starch, 5% saccharose, 4% corn oil, and 1% urea, and then deionized water (DI) was added with the matrix/water ratio of 45/55. The circular film samples with a diameter of 4 cm were buried at a depth of 6 cm. The biodegradation environment was maintained at 58 ± 2 ºC, and DI water was supplemented regularly to maintain the moisture content of the compost. Prior to weighing the film, the waste matrix was meticulously removed from the surface. The mass loss of the films was calculated using the Equation (3).

$$Mass\ loss\ (\%) = \frac{m_i - m_d}{m_i} \times 100\% \quad (3)$$

Where, m_i is the mass of the initial film, m_d is the mass of the film after compost degradation.

The apparent density of the samples was determined according to the general principle of ISO 534:2011. The thickness of 9 cm diameter FP and MFP_{120}-2 sample was measured as single-sheet thickness using a Yuan Heng Tong digital micrometer (YHT127), and the average value from 10 random positions was used for calculation. The dry mass of each sample was measured using an analytical balance, and the apparent density was calculated from the mass and geometric volume. Each sample was tested 10 times, and the reported values represent the mean ± standard deviation.

The life cycle assessment (LCA) of the films was conducted and compared using Simapro 9.5 software through a comparative cradle-to-gate.[9] In this study, the functional unit was defined as the production of 1 kg MFP_{120}-2 Straw. Eleven environmental impact categories were assessed by the ReCiPe 2016 Midpoint method.

Table S1. Sample abbreviations of paper-based materials prepared under different processing conditions.

Sample	Temperature (℃)	Immersion Time (s)
FP	-	-
MFP_{100}-2	100	2
MFP_{100}-6	100	6
MFP_{100}-10	100	10
MFP_{100}-20	100	20
MFP_{110}-2	110	2
MFP_{110}-6	110	6
MFP_{110}-10	110	10
MFP_{110}-20	110	20
MFP_{120}-2	120	2
MFP_{120}-6	120	6
MFP_{120}-10	120	10
MFP_{120}-20	120	20
MFP_{130}-2	130	2
MFP_{140}-2	140	2

FP: pristine filter paper as the control.

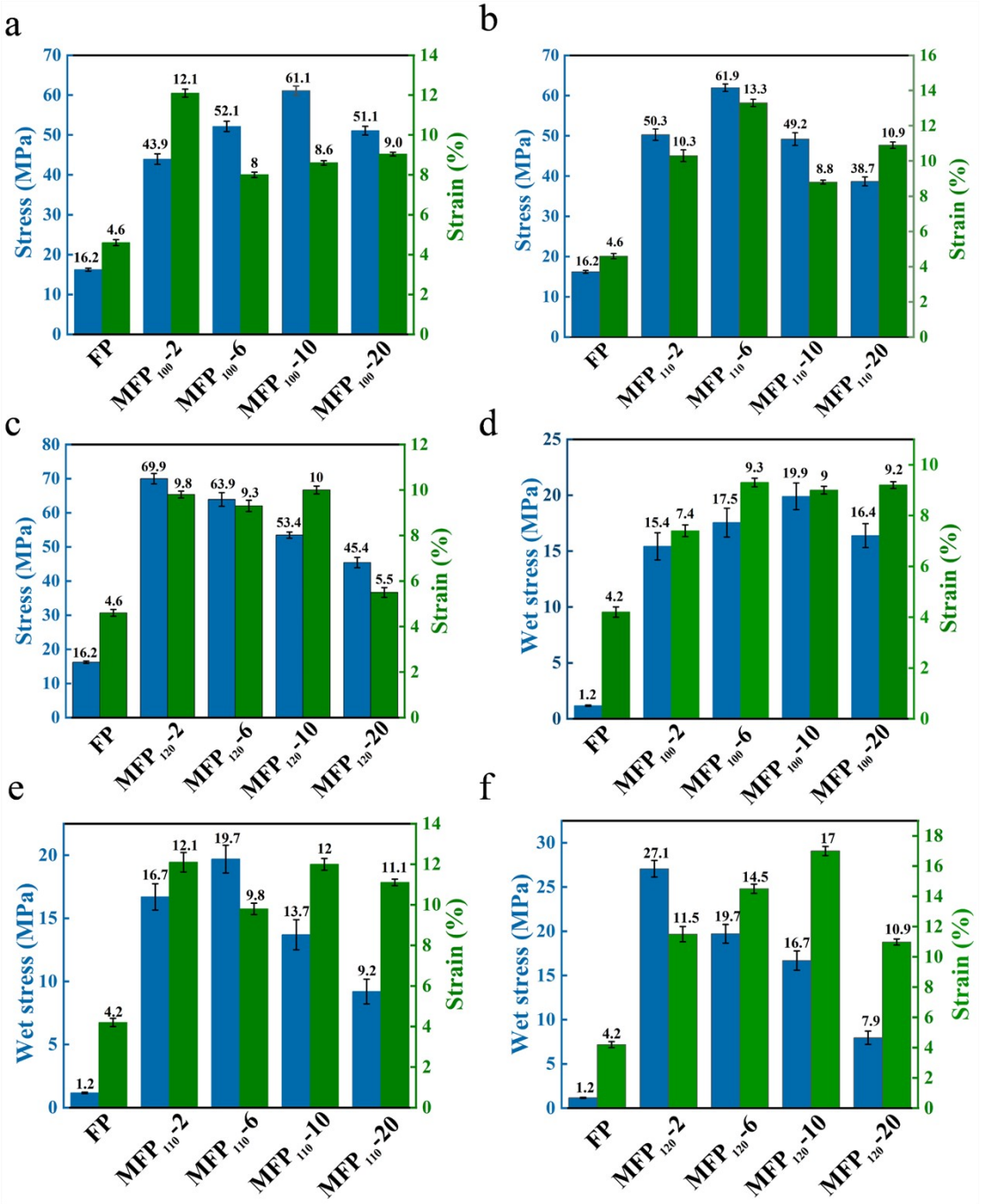

Figure S1. (a–c) Statistical analysis of tensile properties under dry conditions for cellulose-based bioplastics obtained after LBTH treatment at 100 °C (a), 110 °C (b), and 120 °C (c) for different immersion durations. (d–f) Corresponding wet tensile properties measured after water immersion for 24 h.

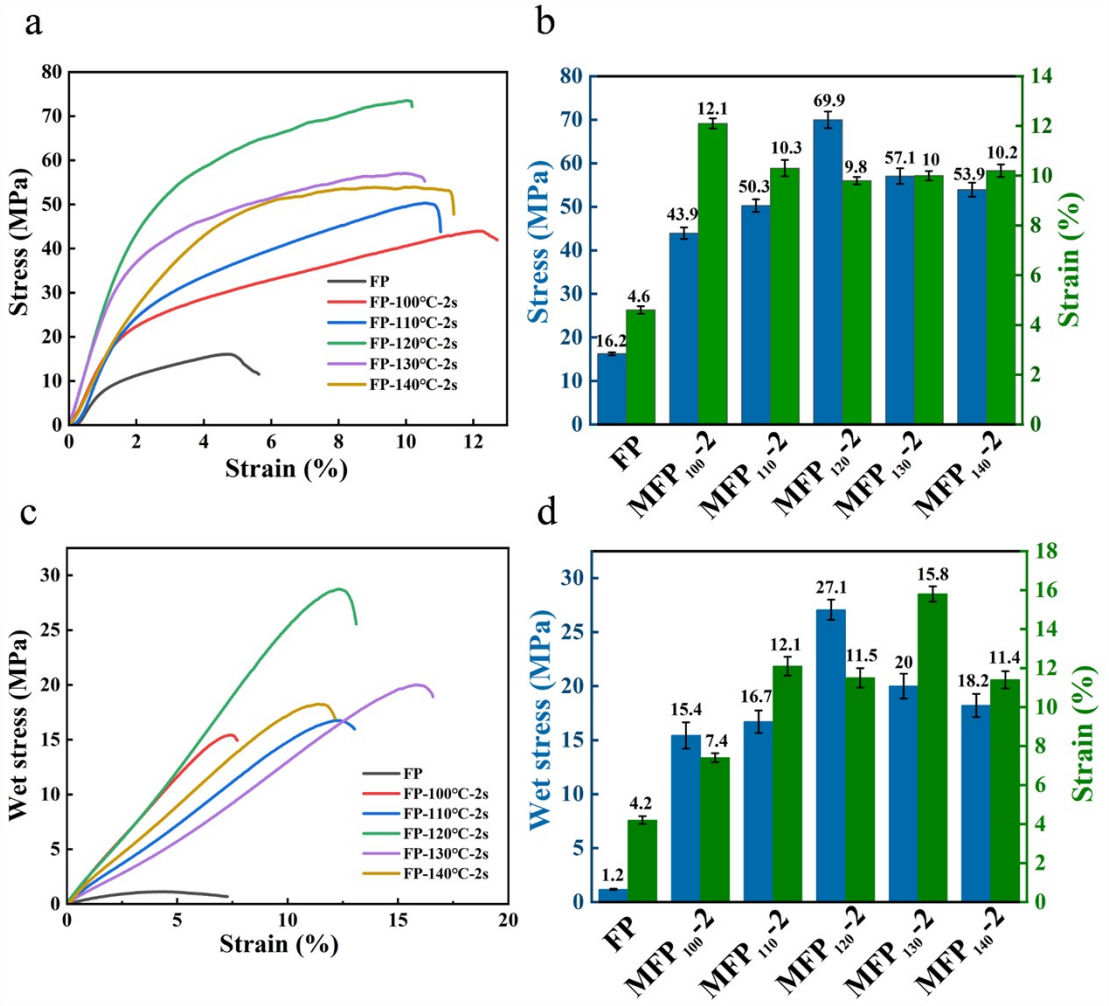

Figure S2. (a, b) Tensile stress–strain curves (a) and corresponding statistical analysis (b) under dry conditions for cellulose-based bioplastics obtained after LBTH treatment for 2 s at different temperatures. (c, d) Tensile stress–strain curves (c) and corresponding statistical analysis (d) measured after water immersion for 24 h.

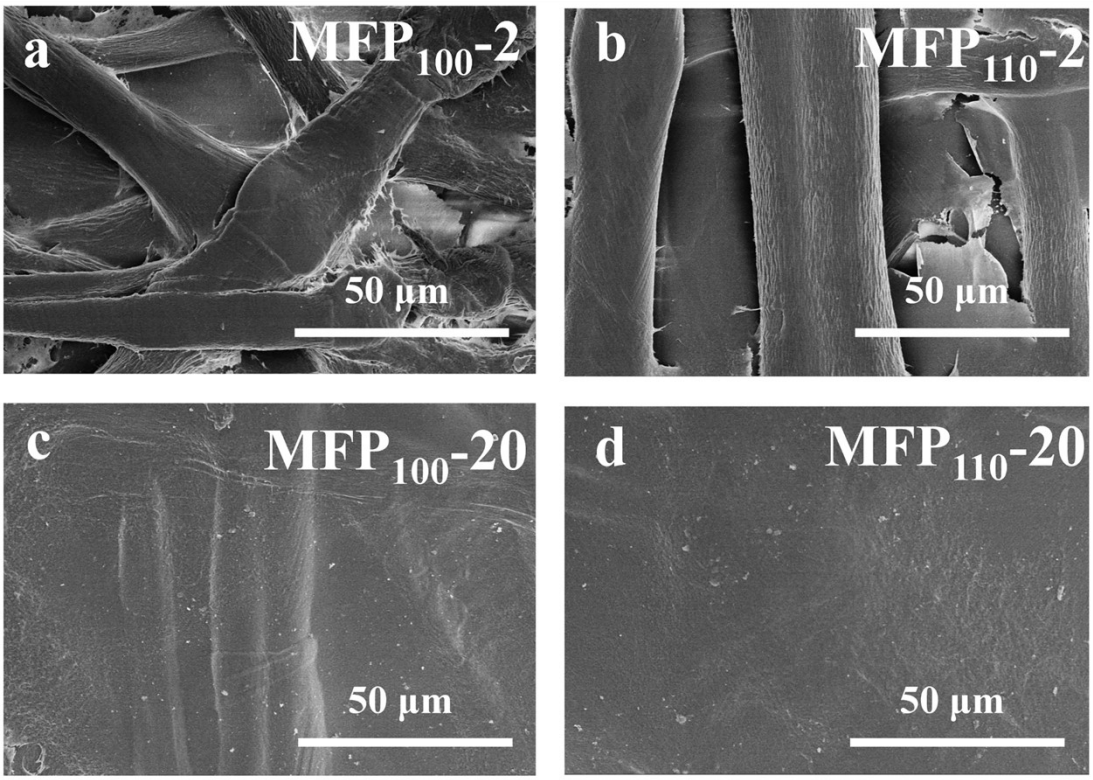

Figure S3. SEM images of MFP_{100}–2 (a), MFP_{110}–2 (b), MFP_{100}–20 (c), and MFP_{110}–20 (d).

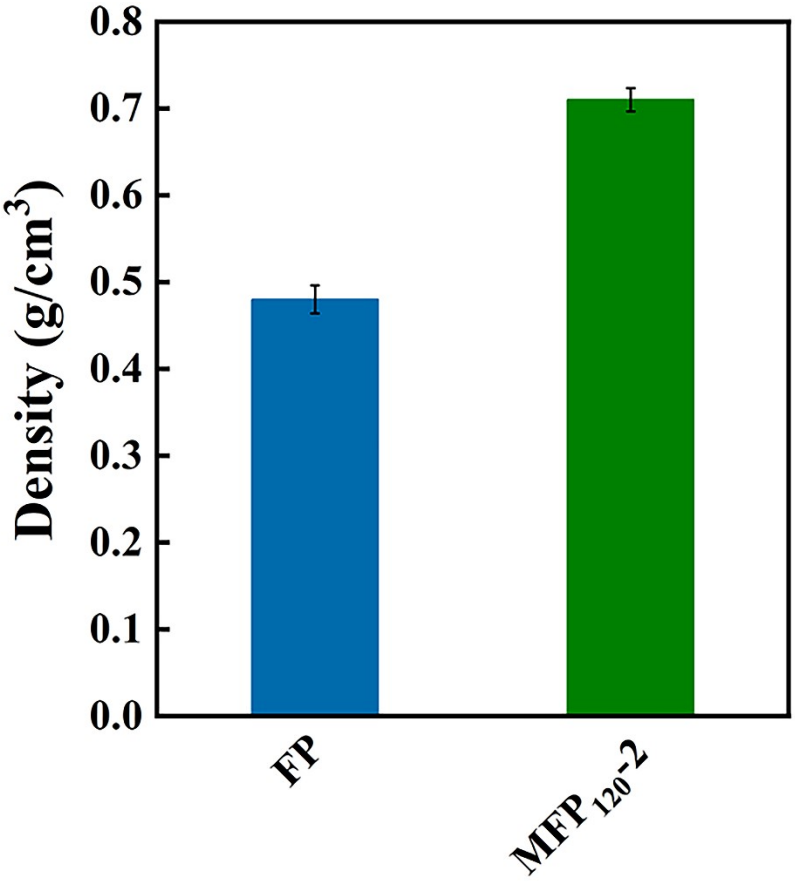

Figure S4. Density of FP and MFP_{120}–2.

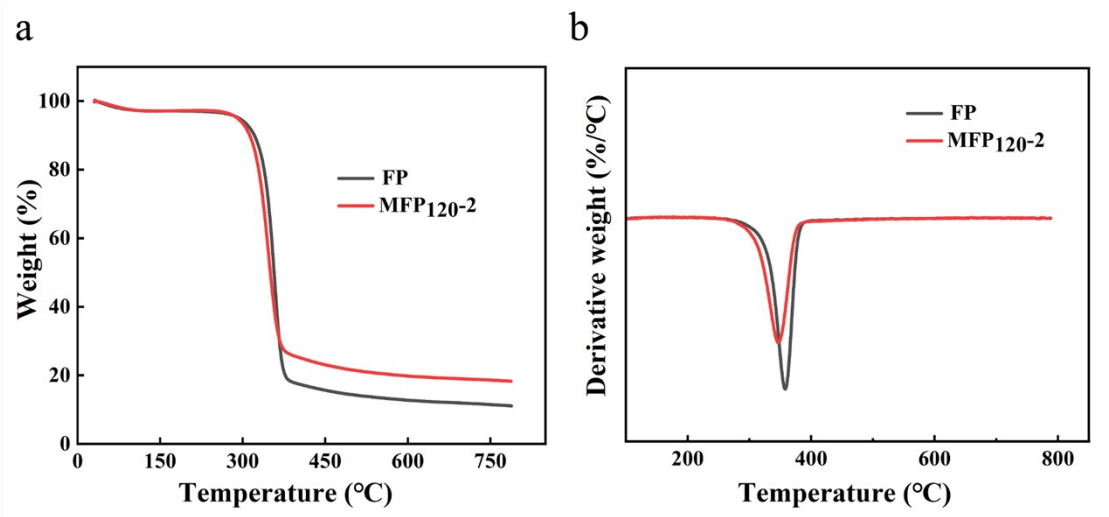

Figure S5. Thermogravimetric analysis (TGA) (a) and derivative thermogravimetric (DTG) (b) curves of FP and MFP_{120}–2.

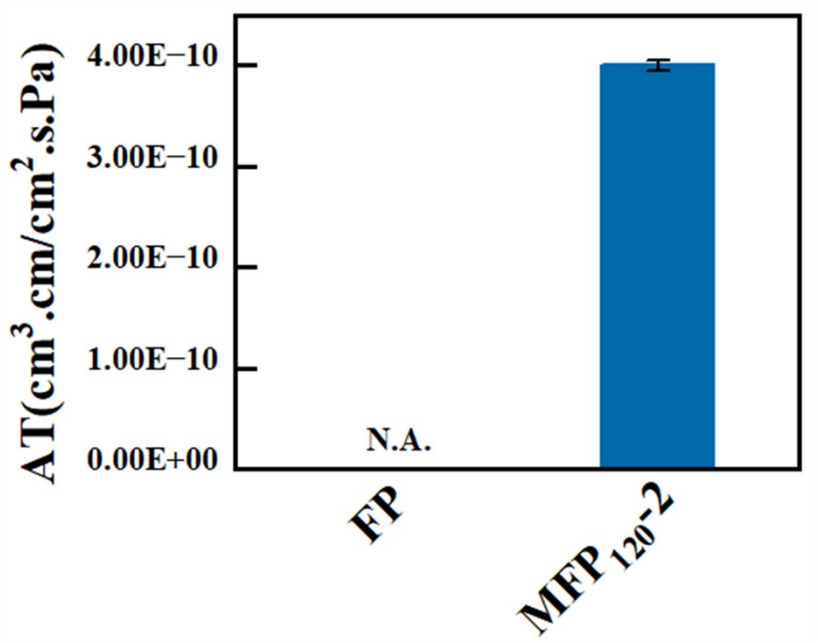

Figure S6. Oxygen transmission rate (OTR) of FP and MFP_{120}–2. *N.A.* indicates not applicable.

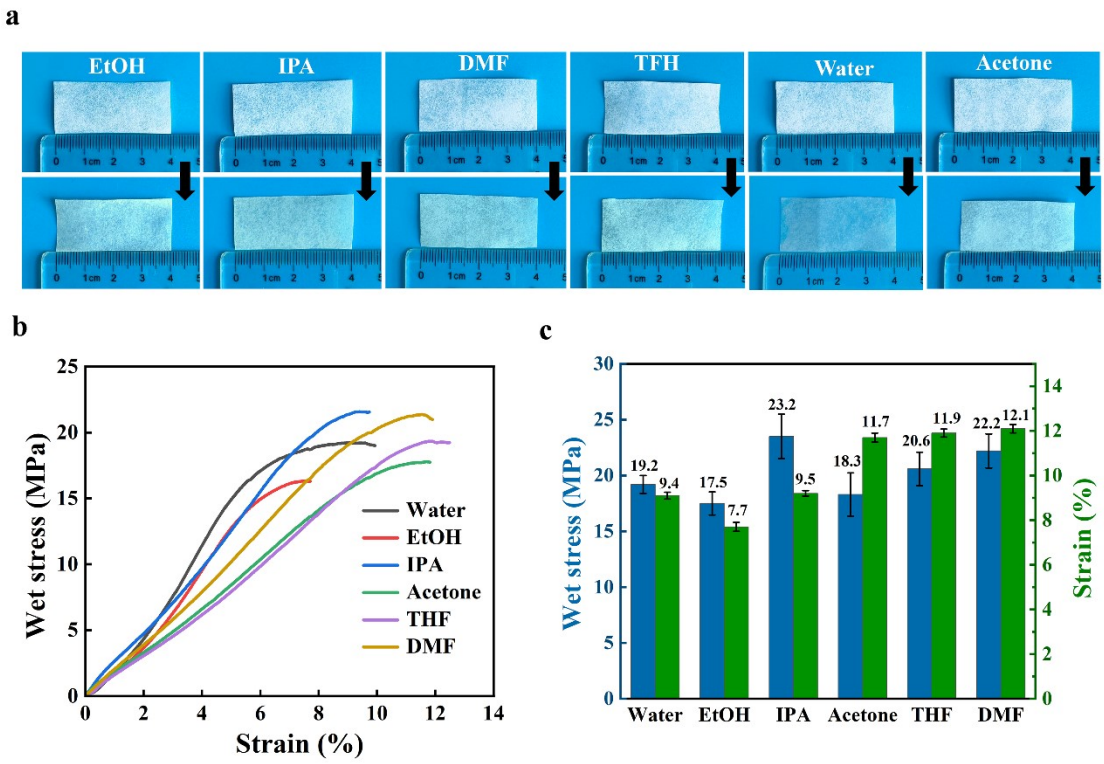

Figure S7. (a) Photographs of MFP_{120}–2 after immersion in different organic solvents for 7 days. (b, c) Tensile stress–strain curves (b) and corresponding statistical analysis (c) of MFP_{120}–2 after immersion in organic solvents for 7 days.

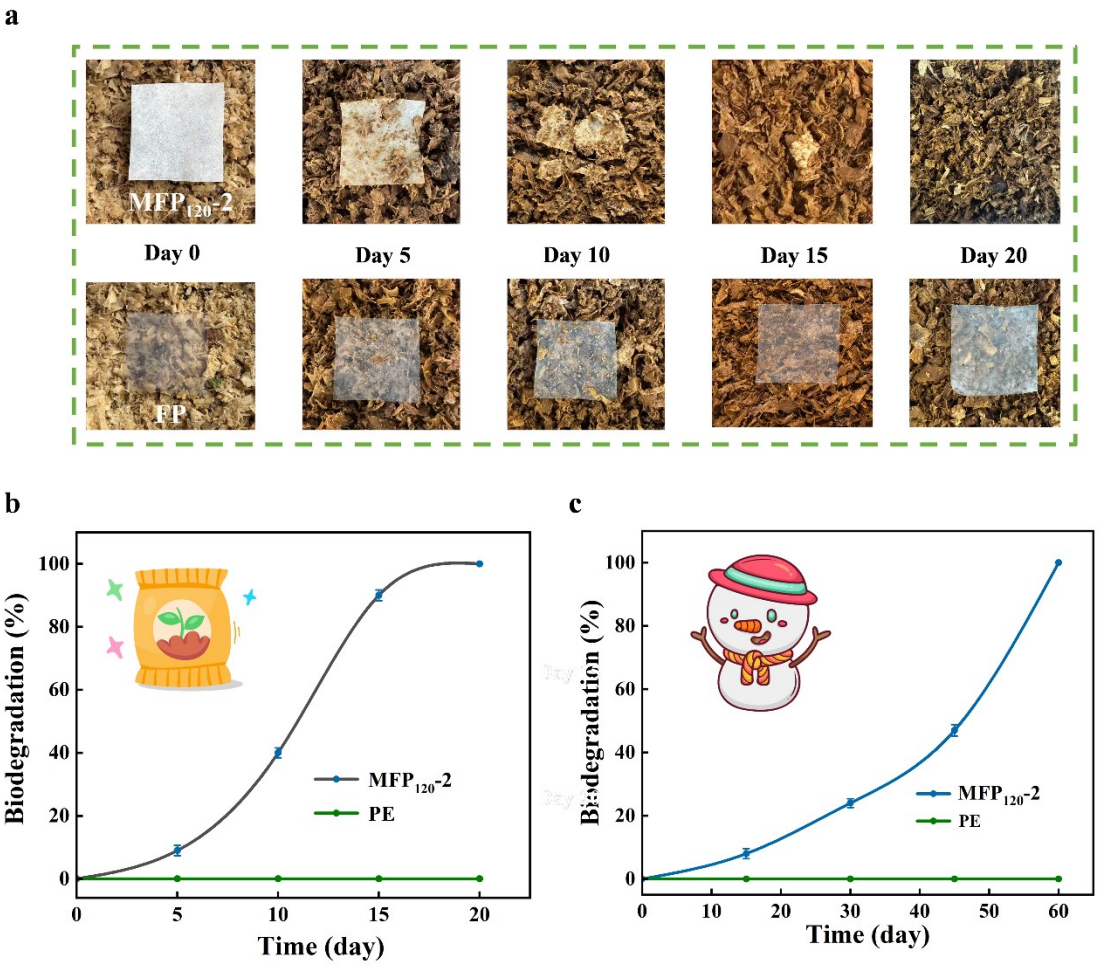

Figure S8. (a) Biodegradation behaviour of MFP_{120}–2 under composting conditions. (b) Biodegradation rate of MFP_{120}–2 under composting and winter landfill conditions.

Figure S9. Liquid uptake performance of the MFP_{120}–2 straw after immersion in water for 4 h, demonstrating retained structural integrity and water stability.

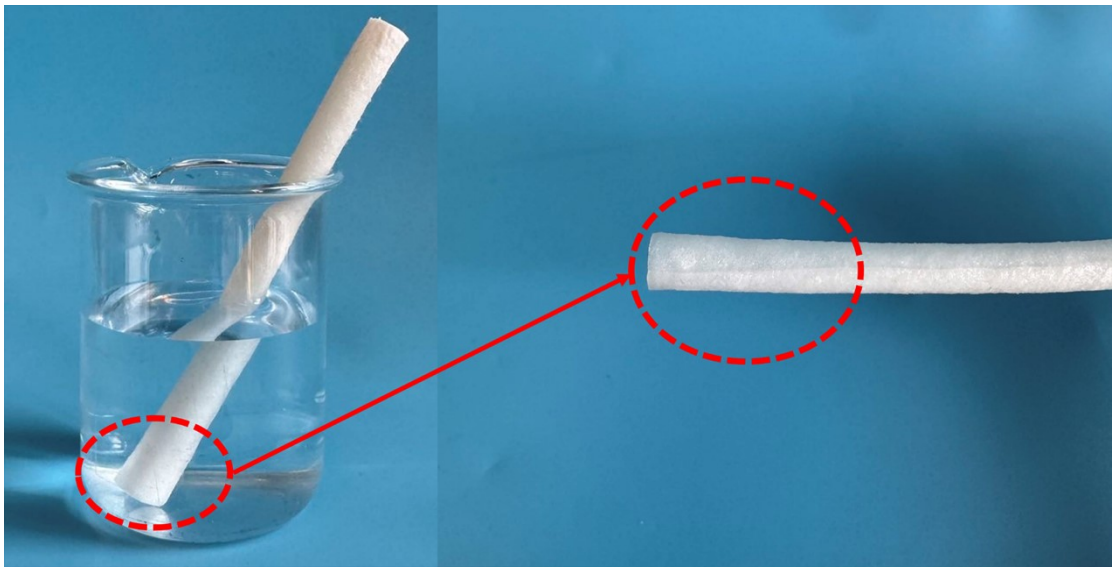

Figure S10. MFP_{120}–2 straws after immersion in water for 2 days, retaining their tubular shape without clear change.

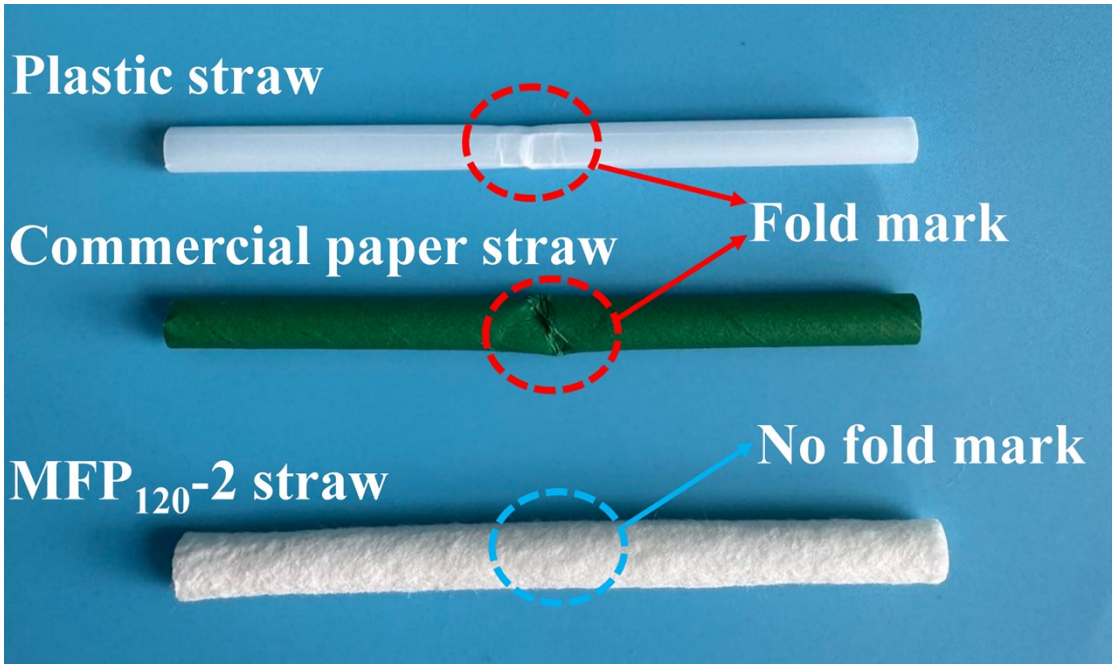

Figure S11. Photographs of different straws after bending deformation. Plastic and commercial paper straws exhibit visible bending marks, whereas the MFP_{120}–2 straw shows no cracking after severe deformation, indicating superior flexibility.

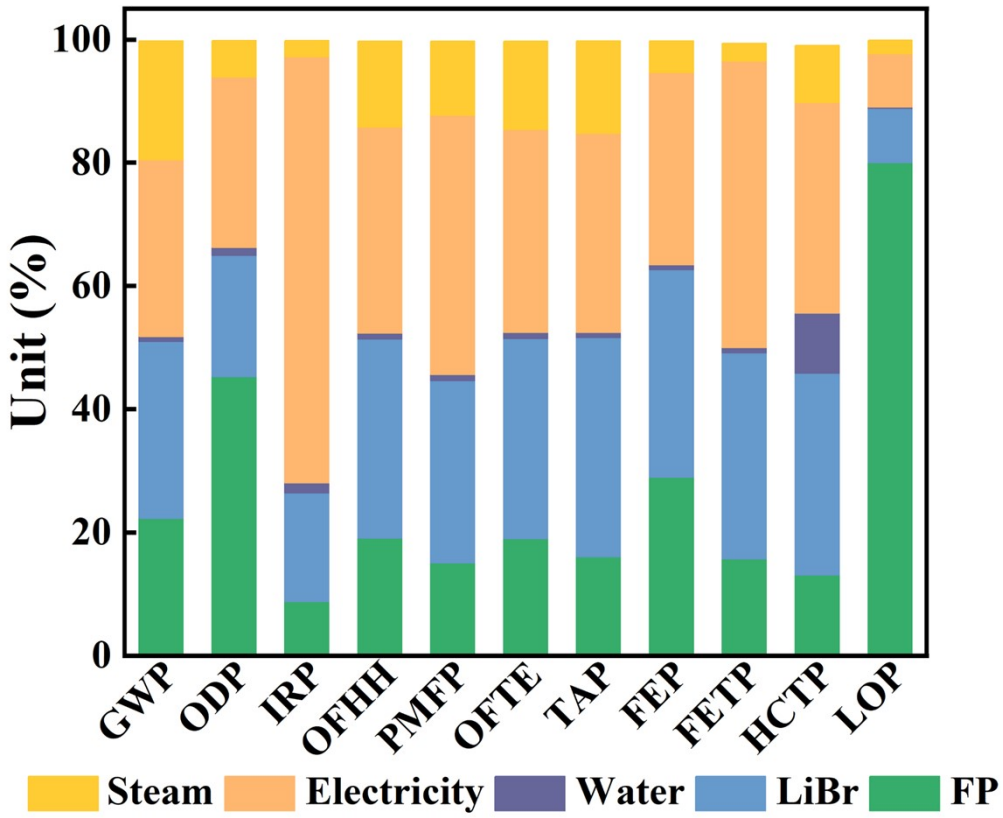

Figure S12. Contribution analysis for 1 kg MFP_{120}–2 straws.

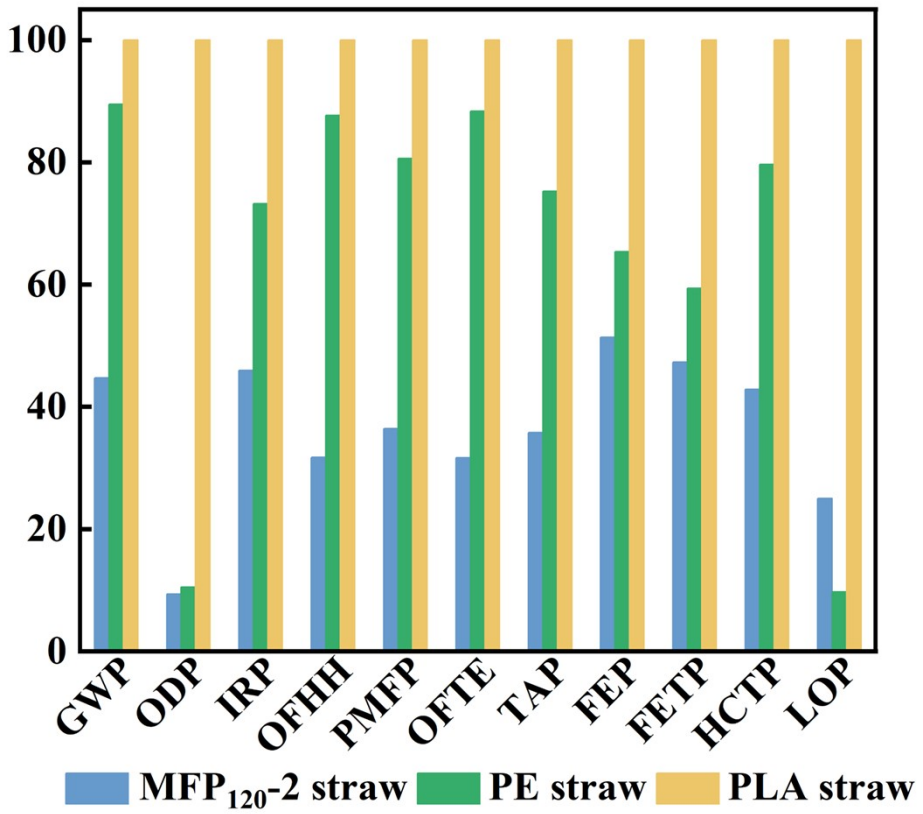

Figure S13. The stage-wise results of environmental impacts of 1 kg MFP_{120}–2 straws.

Table S2. The life cycle inventory data for the production of 1 kg MFP_{120}–2 straws.

Input	Amount	Unit	Source of inventory
Filter paper	1	kg	Ecoinvent v3
Lithium bromide [a)]	0.1	kg	-
Low-pressure steam [b)]	5.2	MJ	Ecoinvent v3
Electricity [c)]	1.34	kWh	Ecoinvent v3
Water	30	kg	Ecoinvent v3
Output	**Amount**	**Unit**	**Source of inventory**
MFP_{120}-2 straw	1	kg	-
Waste water	30.1	kg	Ecoinvent v3

Notes:

[a)] Data on lithium bromide produced from 0.282 kg of lithium hydroxide, 0.95 kg of bromine, and 0.013 kg of liquid hydrogen, where the data for lithium hydroxide, bromine, and liquid hydrogen are all from Ecoinvent v3.

[b)] Low pressure steam is used to recycle lithium bromide solution;

[c)] Electricity is used to operate the oil bath and the hot press;

Supplementary References

1. S. Y. Oh, D. I. Yoo, Y. Shin and G. Seo, *Carbohydr. Res*, 2005, **340**, 417-428.
2. L. Yuan, J. Wan, Y. Ma, Y. Wang, M. Huang and Y. Chen, *BioResources*, 2013, **8**, 717-734.
3. S. Y. Oh, D. I. Yoo, Y. Shin, H. C. Kim, H. Y. Kim, Y. S. Chung, W. H. Park and J. H. Youk, *Carbohydr Res*, 2005, **340**, 2376-2391.
4. L. Segal, J. J. Creely, A. E. Martin and C. M. Conrad, *Text. Res. J.*, 1959, **29**, 786-794.
5. Z. Huang, C. Liu, X. Feng, M. Wu, Y. Tang and B. Li, *Cellulose*, 2020, **27**, 1-14.
6. X. Yang, L. Yu, B. Zhang, Y. Wang, X. Jia, E. Lizundia, C. Chen, F. Dong, L. Qi and L. Chen, *Nat Commun*, 2025, **16**, 6523.
7. Y. Chen, C. Huang, Z. Miao, Y. Gao, Y. Dong, K. C. Tam and H.-Y. Yu, *ACS Nano*, 2024, **18**, 8754-8767.
8. K. Huang, A. Maltais and Y. Wang, *Carbohydr. Polym*. Tech., 2023, **6**, 100391.
9. H. Zhou, Y. Mao, Y. Zheng, T. Liu, Y. Yang, C. Si, L. Wang and L. Dai, *Chem. Eng. J.*, 2023, **471**, 144572.